metals

MDPI

Article

Reuse of Grade 23 Ti6Al4V Powder during the Laser-Based Powder Bed Fusion Process

Ryan Harkin, Hao Wu *, Sagar Nikam, Justin Quinn and Shaun McFadden

Faculty of Computing, Engineering, and Built Environment, Ulster University, Derry/Londonderry BT48 7JL, UK; harkin-r7@ulster.ac.uk (R.H.); s.nikam@ulster.ac.uk (S.N.); jp.quinn@ulster.ac.uk (J.Q.); s.mcfadden2@ulster.ac.uk (S.M.)

* Correspondence: h.wu@ulster.ac.uk

Received: 26 November 2020; Accepted: 18 December 2020; Published: 21 December 2020

Abstract: Titanium alloy powder used for laser-based powder bed fusion (L-PBF) process is costly. One of the solutions is the inclusion of a powder recycling strategy, allowing unused or exposed powder particles to be recuperated post manufacture, replenished and used for future builds. However, during a L-PBF process, powder particles are exposed to high levels of concentrated energy from the laser. Particularly those in close proximity to the melt pool, leading to the formation of spatter and agglomerated particles. These particles can settle onto the powder bed, which can then influence the particle size distribution and layer uniformity. This study analysed extra-low interstitial (ELI) Ti6Al4V (Grade 23) powder when subjected to nine recycle iterations, tracking powder property variation across the successive recycling stages. Characterisation included chemical composition focusing upon O, N, and H content, particle size distribution, morphology and tapped and bulk densities. On review of the compositional analysis, the oxygen content exceeded the 0.13% limit for the ELI grade after 8 recycles, resulting in the degradation from Grade 23 level.

Keywords: selective laser melting; laser-based powder bed fusion; additive manufacturing; powder recycling; powder characterisation; ELI (Grade 23) Ti6Al4V

1. Introduction

The production costs associated with powder feedstock manufacturing processes are high. A practical way to reduce costs associated with the use of powder feedstock is to recycle powder from previous part builds. Without the inclusion of a recycling regime the cost of the powder in the finished part can double [1]. Typically, during the laser-based powder bed fusion (L-PBF) process, only 10–50% of the of the powder within the build volume is utilised [1]. Within this additive manufacturing (AM) process, the powder is consolidated into the final part and the remainder is available for reuse. However, once the powder is exposed to the fabrication environment within the build chamber, its quality is compromised. Hence, the exposed powder (which may not be suitable for particular application) must be verified and reused with care.

Ti-6wt%Al-4wt%V (Ti6Al4V) is an $\alpha + \beta$ alloy, the most popular form of titanium alloy produced. Ti6Al4V is commonly used in the aerospace, medical and automotive industries due to its high strength-to-weight ratio and excellent corrosion resistance properties. Accounting for approximately 45% of the total weight of all titanium alloys shipped worldwide [2]. Ti6Al4V alloy is mainly available in two grades: Grade 5 and Grade 23. Grade 23 is also known as the extra-low interstitial (ELI) grade because the limits on the interstitial elemental components are lower than for Grade 5. Impurities in titanium alloys have an impact upon mechanical properties, particularly oxygen, nitrogen, hydrogen and carbon [3]. Oxygen and nitrogen are alpha stabilisers in Ti6Al4V parts and may increase the rate of martensitic transformation [2]. Therefore reduced levels of oxygen and nitrogen content associated

with Grade 23, allows for improved ductility and fracture toughness properties desired for biomedical and cryogenic applications [4].

Components fabricated by L-PBF are manufactured in a layer-on-layer manner, from a pre-determined computer-aided design (CAD) model. The fabrication process uses a high energy density laser beam to selectively melt particles that have been deposited onto the powder bed by a recoater blade. The recoater blade ensures even distribution and a fixed height of each layer, which typically ranges between 20–60 µm [3]. The recoating and selective melting processes are repeated until the part has been completed. Molten titanium is highly reactive and therefore, in an attempt to reduce reactions with the gases present in the air, the fabrication chamber is purged with argon and the oxygen level typically controlled to be lower than 0.2 wt%.

The condition of the virgin powder properties is associated with the production process. Plasma atomisation is a suitable option for powder production as it produces highly spherical particles [5]. The powders used in L-PBF processes have many stringent technical requirements for morphology, flowability, particle size distribution (PSD), and composition, among others. The morphology must be highly spherical to ensure good powder flowability [6]. Good flowability ensures even spreading during the recoating process. The importance of the PSD for L-PBF process has been evaluated and an average particle size of 10–60 µm is desired [7,8]. Despite the advantages associated with the L-PBF process, on-going challenges remain in relation to the powder material. In addition, the variability of the powder condition when supplied as a batch, remains a concern. In relation to recycling Ti6Al4V powder, interstitial absorption, powder coarsening and continual narrowing of PSD curves during recycling has been shown [9].

The importance of incorporating a powder recycling strategy is critical to improving sustainability. Hence, there are two common recycling methods utilised within the L-PBF fabrication processes: single batch and top-up [10,11].

A single-batch recycling strategy involves the depletion of a batch quantity of powder, to complete a series of manufacturing builds without replenishing. Post fabrication unused powder is sieved, to remove agglomerates, contaminants and oxidised particles [12]. The sieved powder is then reintroduced back into the L-PBF. This is repeated until insufficient powder quantities are available from the batch to complete any further build cycles.

The process flow for a top-up recycling procedure is outlined in Figure 1. Post processing, breakout of the parts upon the substrate occurs and any unused powder is retrieved to be sieved. A sample can then be taken for powder analysis to evaluate the build-to-build impact upon the powder quality due to exposure within the processing environment. The exposed powder is replenished and blended with virgin powder, known as 'top-up'. The topped-up powder is reintroduced back into the L-PBF machine for fabrication. This is repeated until the quantity of virgin powder available for replenishing along with the reused powder has been depleted below the fabrication specified requirement.

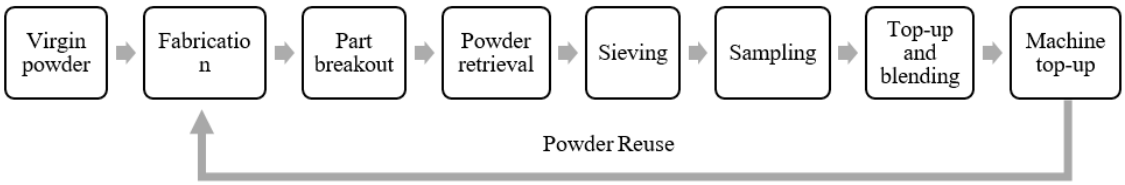

Figure 1. Schematic illustration of the inclusion of a top-up powder recycle regime within the laser-based powder bed fusion (L-PBF) process.

Several studies have reported an impact upon the Ti6Al4V powder condition as a result of recycling [9,10]. Santecchia et al. [1] have reviewed Ti6Al4V powder reuse in L-PBF process. For ease of reference the main works in this area have been summarised in Table 1. It has been shown through characterisation tests that powder properties such as the chemical composition, PSD and particle morphology can be affected [9]. Interstitial absorption, particularly of oxygen and nitrogen has been

reported despite fabrication under an inert atmosphere [13]. The investigations consistently report that powder variation can occur, despite of the recycling strategy. An increase to both oxygen and nitrogen content occurred. The study by Thejane et al. [4], investigated both recycling strategies: top-up and single-batch. It should be noted that two individual L-PBF systems have been reported. From virgin state to 10 recycle iterations using the single batch strategy, the oxygen content (wt%) within ELI Ti6Al4V increased from 0.082% to 0.13%. In comparison with implementation of the top-up strategy, after 25 recycle iterations the oxygen content (wt%) valued at 0.11% with the potential for further recycles. In addition, conflicting reports in relation to the behaviour of the PSD of recycled powder have been reported [14]. However, improved powder flowability was continuously reported due to the reduction of smaller particles, lower moisture content and the absence of satellites [15,16].

Table 1. Previous studies into the recycling of Ti6Al4V powder within the L-PBF process, the recycling strategy used, factors investigated and number of powder reuse times.

Reference	Recycling Strategy	Factors Investigated/Limitations	Reuse Times
Seyda et al. [18]	Single batch	PSD broadened, particles coarsened, flowability improved, compositional analysis not performed	12
Quintana et al. [14]	Single batch	PSD narrowed, oxygen content limit reached, flowability improved	31
Carrion et al. [13]	Single batch	PSD narrowed, flowability improved, oxygen and nitrogen increased, separate batches were utilised	15
Cordova et al. [10]	Single batch	No significant change to PSD, changes in oxygen content measured but within measurement uncertainty, flowability improved	11
Denti et al. [17]	Top-up	PSD narrowed, oxygen content increased (data was not provided), tests limited due to amount of powder available	100
Thejane et al. [4]	Single batch	Smaller particle sizes, spherical particles	10
Thejane et al. [4]	Top-up	PSD broadened with a shift towards a smaller particle sizes, spherical particles, potential for further recycles	25
Park et al. [19]	Single batch	PSD narrowed, 0.13 wt% oxygen content reach at 20th cycle, flowability improved	38

Research performed to date has primarily focused upon the single-batch method. It is critical however to evaluate the top-up recycling strategy as this reflects industrial practice. The inclusion of the replenishing process (addition of virgin powder), within the top-up method, has been shown to reduce the rate of interstitial absorption per recycle [4,17]. However, the presence of batch variation at the virgin state can impact upon the longevity of the powder. Therefore, it is imperative not only to characterise the powder throughout a manufacturing process but also the initial quantity of virgin powder to be used for fabrication. This work will provide a detailed analysis of ELI Ti6Al4V powder during the L-PBF process from virgin state, with the inclusion of a top-up recycling strategy.

Aims and Objectives

The aim of this study is to perform a comprehensive analysis of the condition of ELI Ti6Al4V powder as it is processed through the L-PBF process and maintained using a top-up recycling strategy. The specific objectives include:

1. Tracking of the levels of interstitial elements O, N and H (wt%) at each build stage during the top-up regime.
2. Monitoring and recording of the PSD and particle morphology.
3. The evaluation of the impact of recycling on the flowability of the powder.
4. Critical evaluation of the present findings to those found elsewhere in literature.

2. Materials and Methods

2.1. Process Parameters

L-PBF Fabrication was performed using an MLab Cusing R machine (GE Additive, Lichtenfels, Germany) which has an 80 mm × 80 mm × 90 mm build chamber. Printing was performed upon an industry standard substrate for titanium alloy components. Gravimetrically, the supply chamber had a maximum powder capacity of 3.71 kg. The processing parameters that were selected used consistently throughout, were; laser power: 95 W; layer thickness: 0.025 mm; scanning speed: 900 mm/s and beam size. The focused beam diameter was approximately 50 µm and the hatch spacing was measured as 100 µm. Fabrication was performed within an argon enriched atmosphere, where the oxygen levels were expected to be kept below 0.1%.

2.2. Component Geometry

This research was performed as part of a wider research project; hence the geometry of parts changed from cycle to cycle. It was deemed important to record information relating to the geometry of the part being built and to compare the build volume to overall build chamber volume. Two types of build geometries were considered, namely, pillar builds (P) and test-part builds (T). Pillar builds (shown in Figure 2a) consisted of a single pillar in the middle of the platform. All pillars had a consistent height of 70 mm, but their diameters (D) varied at each cycle instance. Test-part builds consisted of an arrangement of cylinders and cuboids (shown in Figure 2b).

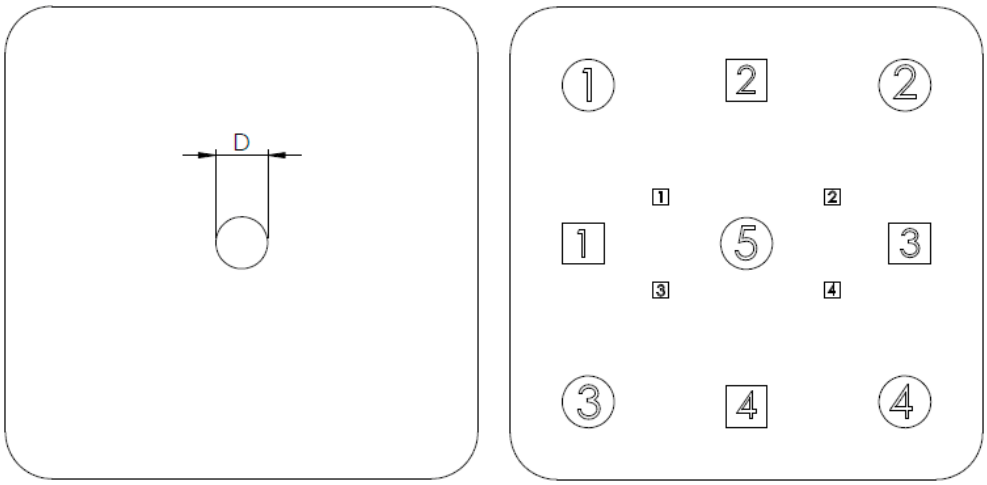

(**a**) (**b**)

Figure 2. Top view of a (**a**) pillar build and (**b**) test-part build showing the position of the components on the build plate.

Table 2 shows the ratio of the final volume of the built components, v, in each cycle to the overall volume of the build chamber, V. Since all parts were prismatic, the volume ratio is representative of the scanned area fraction at each layer.

Table 2. Geometric volume ratios and geometry type for each cycle. P, represents pillar build and T, represents test-part geometry.

Cycle	**1**	**2**	**3**	**4**	**5**	**6**	**7**	**8**	**9**	**10**	**11**	**12**
Type	P	T	T	P	T	P	T	P	T	T	T	T
v/*V*	0.01	0.05	0.05	0.04	0.05	0.09	0.05	0.06	0.05	0.05	0.05	0.05

2.3. Feedstock Powder

Plasma-atomised ELI Ti6Al4V powder (Carpenter Additive, Widnes, UK) was utilised throughout this study. A 40 kg 'master batch' of powder was received along with a mill certificate. This master batch was supplied in unit 2.5 kg batches (×16) air-tight containers with desiccant included to absorb moisture. The PSD for the virgin powder within the master batch, was based upon the average volume laser size diffraction method and ranged between 14.5–76 µm. Approximately 85% of the particles ranged between 25–50 µm.

2.4. Preparation of Control Pot

The mill certificate of the 40 kg master batch was deemed useful but insufficient to represent the condition of the powder at cycle 0. A 2.5 kg unit batch of powder (test pot) was characterised upon receipt. To fulfil the powder requirement of the machine, 2.26 kg (0.24 kg sample taken for chemical compositional analysis) from the test pot along with 1.29 kg from the master batch was mixed and referred to as the 'control pot'. The powder handling process to determine the control pot is provided within Figure 3. It was assumed that the powder characterisation performed on the 150 g sample taken from the control pot, was representative of the remaining 3.40 kg powder entered into the L-PBF machine for the initial fabrication (cycle 0).

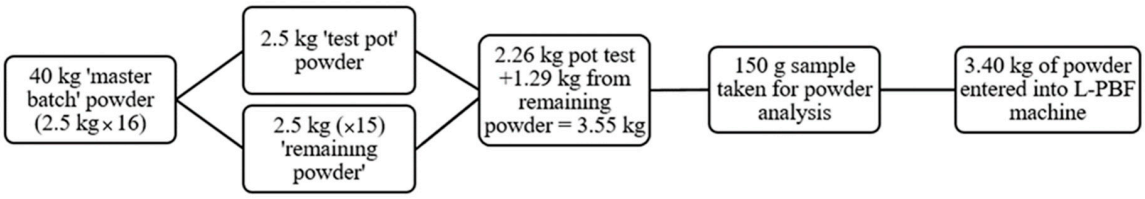

Figure 3. Preparation procedure for the virgin powder within the control pot at cycle 0.

2.5. Powder Recycling

A detailed process flow of the top-up recycling strategy implemented throughout the experimental regime presented in Figure 4. After each fabrication stage, unused powder was sieved in a two-stage (63 µm and 50 µm) process using a mechanically vibrating Retsch AS 200 sieve (Retsch GmbH, Haan, Germany) at amplitude of 60 Hz for 600 s. After sieving a 200 g sample of powder was then taken via grab sampling for characterisation. The powder was then topped-up and blended with virgin powder from the master batch, to a quantity of 3.71 kg. Blending was performed by the sieve using the 63 µm mesh. Finally, the powder was entered into the supply chamber of the L-PBF machine for the subsequent fabrication process.

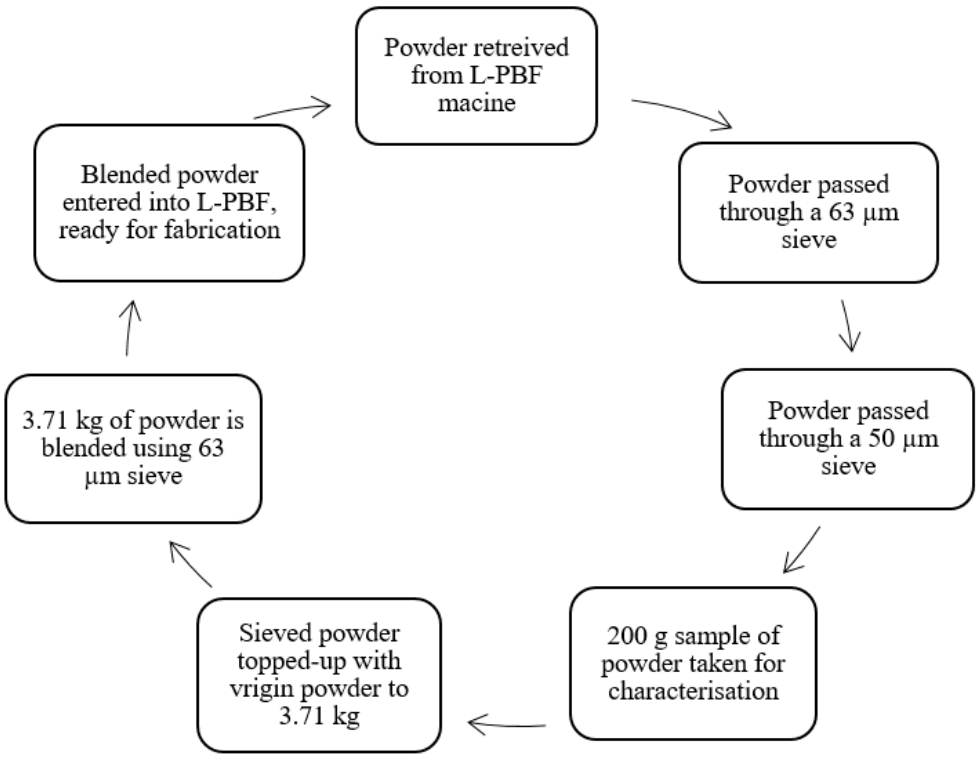

Figure 4. Procedure for top-up of powder for all cycles after the initial build.

2.6. Powder Characterisation

The powder characterisation tests performed are summarised with Table 3. In relation to the test occurrences, 0–9 represents all cycles from zero to nine for example. Whereas, 0, 3, 7 refers to characterisation at selected cycles only. Chemical composition analysis was determined by inert gas fusion (IGF), which provided oxygen, nitrogen and hydrogen interstitial elements compositions (wt%). The measurement uncertainty of the test apparatus was 5% for oxygen at 0.1% and 25% for nitrogen at 0.02%. The PSD was determined by a Mastersizer 3000 (Malvern Panalytical, Worcestershire, UK) using the laser size diffraction (LSD) technique. Both volume and number weighted distribution was reported and the data was analysed in triplicate, with an average determined. The morphology was determined by scanning electron microscopy (SEM), providing qualitative images of the powder particles taken at magnifications of 300, 500 and 1000. Quantitative shape analysis was acquired via optical analysis of 10,000 particles evenly dispersed over a glass slide.

Table 3. Powder characterisation method utilised and the occurrence of tests performed.

Characterisation Method	ASTM/ISO Standard	Test Method	Test Occurrence (Cycle)
Chemical composition	ISO 17025	O, N and H analysis	0–9
Sizing	ASTM B822	Laser size diffraction (volume and weighted number distribution)	0–9
Bulk morphology	-	SEM morphology imaging	0, 3, 7
Powder morphology	-	Quantitative shape analysis	0, 3, 7
Density	ASTM B212	Apparent density	0–9
Density	ASTM B527	Tap density	0–9
Flowability	ASTM B213	Hall flow rate	0–9
Moisture	ASTM E1868	Moisture content	0, 3, 7

Bulk density, which is defined as the mass per unit volume (g/cm^3) of a powder after being subjected to free fall, was measured. Tap density, which is the mass per unit volume (g/cm^3) of a powder after being vertically agitated until no more visible settling occurs, was also measured at the cycles mentioned in Table 3. Both tests were analysed in triplicate and an average was determined. The Hausner ratio (H_R) and Carr's compressibility index (C_I) are defined as the ratio and relative difference between the bulk density (V_o) and the tap density (V_f), as shown in Equations (1) and (2), respectively. Flowability was measured by the Hall flow method. This characterisation technique calculated the time taken for 50 g of powder to discharge through a Hall flowmeter and was expressed as time per mass unit (s per 50 g). The Hall flow tests were analysed in triplicate and an average was determined. Moisture content within the powder was measured using the loss-on-drying technique. The powder was heated with a 180 °C filament for 90 s, with the change in weight (g) after drying considered as the moisture content (wt%).

$$H_R = \frac{V_f}{V_o}, \quad (1)$$

$$C_I = \frac{100\ (V_f - V_o)}{V_f}, \quad (2)$$

3. Results

3.1. Chemical Compositional Analysis

The nominal composition and the measured chemical compositional analysis of the virgin ELI Ti6Al4V powder is reported within Table 4.

Table 4. Chemical composition (wt%) of ELI Ti6Al4V powder within the master batch, test pot and control pot (cycle 0).

Element	Al	V	Fe	C	O	N	H	Ti	Other	All Other
Grade 23 min	5.5	3.5	-	-	-	-	-	-	-	-
Grade 23 max	6.5	4.5	0.25	0.03	0.13	0.03	0.012	Bal	0.1	0.4
Master batch	6.4	4	0.19	0.01	0.07	0.01	0.001	Bal	<0.1	<02
Test pot	6.5	4	0.19	0.02	0.11	0.01	0.003	Bal	<0.1	<0.2
Control pot	-	-	-	-	0.095	0.014	0.002	-	-	-

Chemical compositional analysis on the oxygen, nitrogen and hydrogen content was performed upon the powder throughout nine recycling iterations. The results of the oxygen content are presented in Figure 5, with nitrogen and hydrogen content shown in Figure 6. Most notably, the average oxygen content of the tests performed at cycle 8 exceeded the Grade 23 limit (ASTM F13-136). In relation to the nitrogen and hydrogen content, the levels remained below the thresholds of 0.03 wt% and 0.012 wt% respectively, throughout all recycling cycles.

3.2. Sizing—Particle Size Distribution

The PSD results reported in Table 5 were classified in relation to Dv_{10}, Dv_{50} and Dv_{90} values. For example, the Dv_{90} parameter signifies the particle size relating to the 90% percentile of powder on a volume basis (i.e., 90% by volume of the powder is below D_{v90}. The powder was also classified in relation to the number of fine (<14.5 μm) and coarse (>45.6 μm) particles. There were no significant changes for all results throughout all cycles.

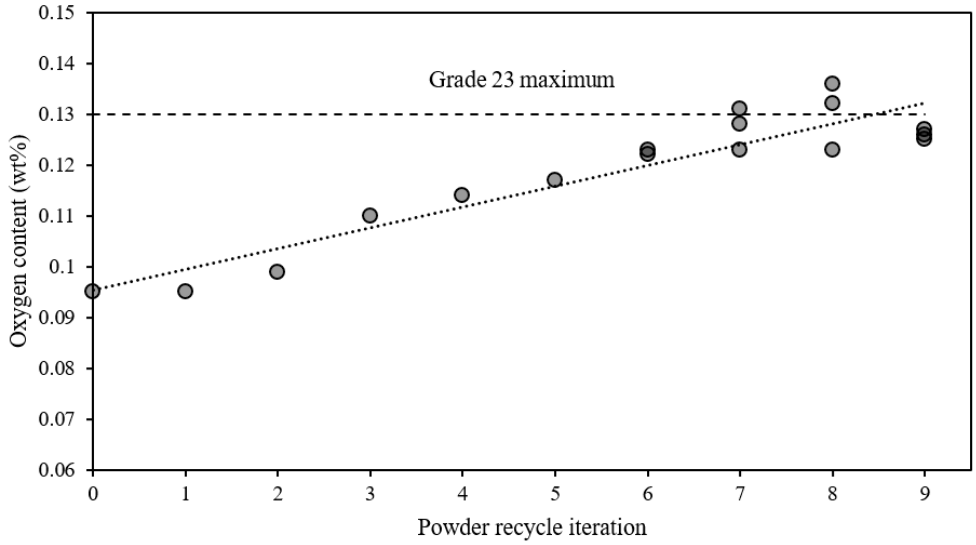

Figure 5. Oxygen content within ELI Ti6Al4V powder at each powder recycle iteration.

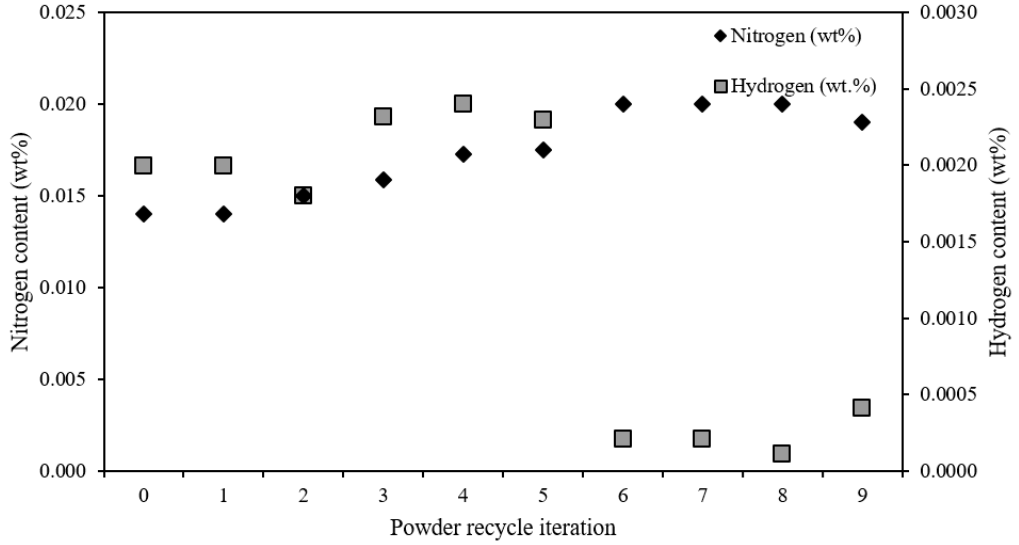

Figure 6. Nitrogen and hydrogen content (wt%) within ELI Ti6Al4V powder at each powder recycle iteration.

Table 5. Dv10, Dv50 and Dv90 values of the ELI Ti6Al4V powder across nine cycles of a top-up recycle strategy.

Analysis	**Cycle**									
LSD	0	1	2	3	4	5	6	7	8	9
Dv10	22.3	21.8	22.2	21.6	21.8	21.6	21.9	22.1	21.8	22.5
Dv50	33	32.4	32.6	32.2	32.4	32.2	32.4	32.6	32.1	33.1
Dv90	48.3	47.6	47.4	47.3	47.7	47.5	47.2	47.6	46.8	48.2
<14.5 µm	0.06	0.09	0.05	0.12	0.09	0.13	0.07	0.05	0.08	0.03
14.5–45.6 µm	86.34	87.38	87.67	87.84	87.31	87.5	88.04	87.45	88.52	86.51
>45.6 µm	13.6	12.53	12.28	12.04	12.6	12.37	11.89	12.50	11.40	13.46

Figure 7 displays the particle size distribution curve (probability density function) and the cumulative frequency for the ELI Ti6Al4V powder, comparing cycle 0 (virgin powder), cycle 7 and cycle 9. Additionally, there was no obvious narrowing of the PSD curves at cycle 9.

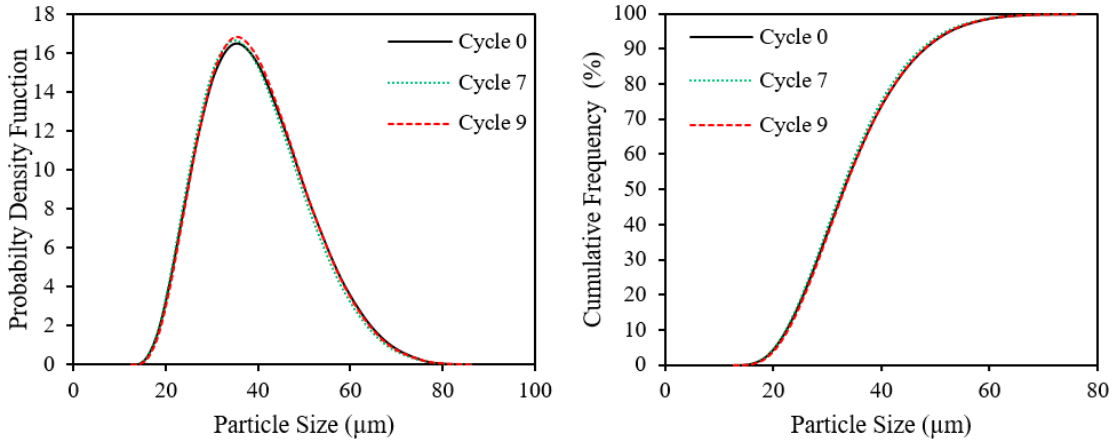

(**a**) (**b**)

Figure 7. (**a**) PSD and (**b**) cumulative frequency curves of the ELI Ti6Al4V powder, comparing cycle 0, cycle 7 and cycle 9 powder.

3.3. Bulk Morphology

SEM images of the powder particle surface features and morphologies were taken at 300×, 500×, 1000× magnifications as displayed in Figure 8. The images show highly spherical powder properties with the presence of satellites in both powder conditions, as pointed by the red arrows.

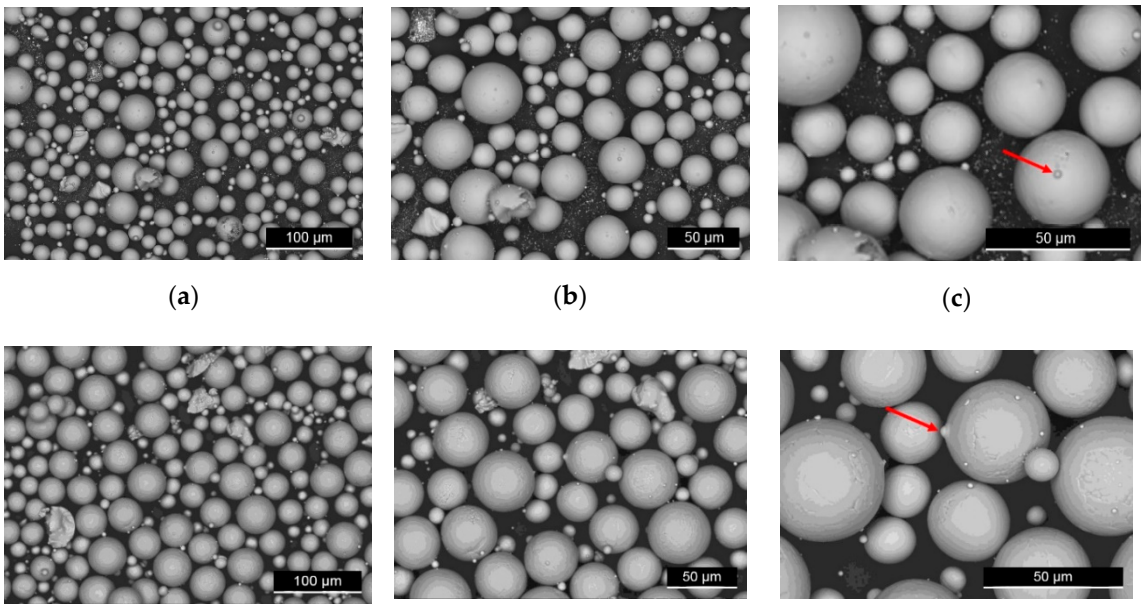

(**a**) (**b**) (**c**)

(**d**) (**e**) (**f**)

Figure 8. SEM images of cycle 0 (upper row) and cycle 7 (lower row) powders at 300× (**a**,**d**), 500× (**b**,**e**), and 1000× (**c**,**f**) magnifications, respectively. Arrows show the presence of satellites.

Particle shape analysis was performed upon cycle 0 and cycle 7 topped-up powder and is provided in Table 6. The mean and relative standard deviation (RSD) was reported for each form of shape analysis.

Table 6. Particle shape analysis of the ELI Ti6Al4V powder at virgin state and cycle 7.

Analysis	Circularity		Convexity		Elongation		CE Diameter (μm)		Aspect Ratio		Solidity	
Powder	**Mean**	**RSD (%)**	**Mean**	**RSD (%)**	**Mean**	**RSD (%)**	**Mean**	**RSD (%)**	**Mean**	**RSD (%)**	**Mean**	**RSD (%)**
Cycle 0	0.971	6.651	0.995	1.660	0.052	152.140	20.79	59.29	0.948	8.380	0.995	1.810
Cycle 7	0.970	6.925	0.995	1.510	0.056	155.590	22.18	45.91	0.944	9.210	0.994	1.930

3.4. Flowability

The Hall flow rate (HFR) tests indicated that improved powder flow occurred due to recycling. At cycle 0 the HFR value was 30 s pre 50 g compared with 23.6 s per 50 g at cycle 9. Figure 9 shows the results of the Hausner ratio (H_R) and Carr's compressibility index (C_I) for nine cycles. Included on the graph are the upper and lower limits of the good flow characteristic for both H_R (1.12–1.18) and C_I (11–15). A decrease to both H_R and C_I was observed from cycle 0 to cycle 9, signifying improved powder flowability during recycling. The moisture content, measured using the loss-on-drying technique, remained stable throughout. It measured 0.4 wt% at cycle 0 and at cycle 7, with a slight increase to 0.42 wt% at cycle 4.

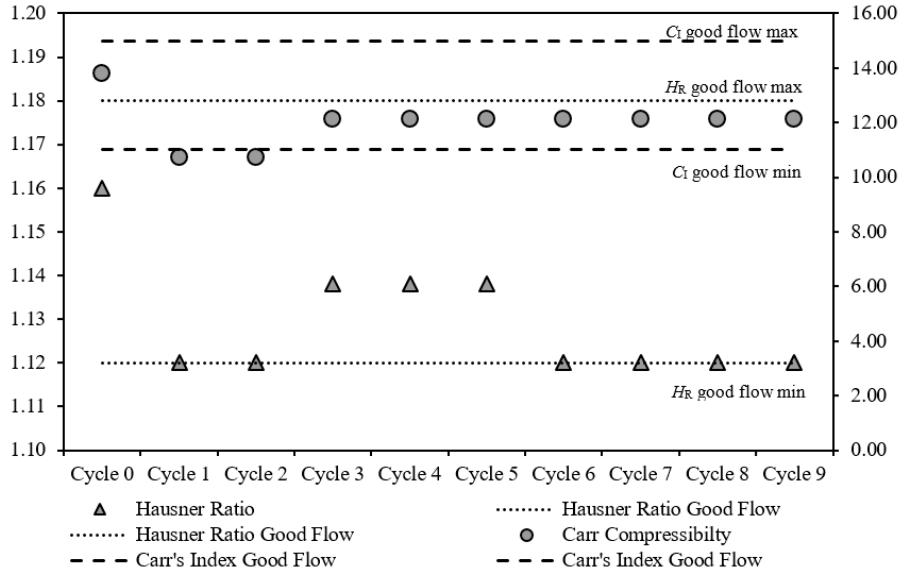

Figure 9. Powder flowability analysis via the Hausner ratio (H_R) and Carr's compressibility index (C_I) at each powder recycle iteration.

4. Discussion

The oxygen content within the ELI Ti6Al4V powder appeared to have increased during recycling. To determine the statistical significance, a regression model was established for the oxygen content versus each cycle iteration. The regression model was linear (see Figure 5) with a slope of $B_1 = 0.004$ and an intersection of $B_0 = 0.096$. The p-value for the slope of the line was 7.84×10^{-8} and R-square value was 0.862. Since this p-value is less than 0.05, the trend in the results can be deemed significant. In addition, the average oxygen content (wt%) at cycle 8 reached the maximum acceptable oxygen content (wt%) level of 0.13 wt% permitted under the ASTM F136-13 for Grade 23. With three data points between cycle 7 and 8 exceeding the Grade 23 threshold value. No reliable trend can be established for the nitrogen and hydrogen compositions. The H_R and C_I values of N and H were comfortably below the threshold values for each component in all cases. Certain limitations are acknowledged within this study. An increase in the number of powder samples taken at each recycle iteration would be advantageous along with additional samples at increased cycle iterations; nevertheless, the trend presented here is statistically significant ($p < 0.05$).

Many studies into the recycling of Ti6Al4V powder within PBF processes have been reported within Table 1. A study by Denti et al. has reported 100 top-up recycle iterations [17]. However, the oxygen content within the powder was not reported. If the trend presented in this study can be accepted, it is unlikely that a top-up recycling strategy could support as many cycles as 100 cycles.

Previous studies investigating recycling of ELI Ti6Al4V powder, have reported narrowing of the PSD curve after 16 recycle iterations [9]. On review of the PSD curves presented within Figure 6, no clear change to the PSD occurred during powder recycling. The particle size measurement Dv_{50} remained practically constant (from 33 µm to 33.1 µm) when comparing virgin and post recycled powder. In addition, a powder recycling study performed by Tang et al. have reported an increase from 72.7 µm to 73.2 µm after the 2nd and 16th recycling iterations [9]. Regarding the number of coarse particles (>45.6 µm), a slight reduction from 13.6% to 13.46% volume under was observed from virgin to 9 times recycled powder. On further analysis of the particle sizes, the number of fine particles (<14.5 µm) as volume (%) has reduced from 0.06% to 0.03%.

The SEM images within Figure 7 shows highly spherical powders particles for each condition, as expected for plasma atomised powder. Higher powder sphericity has also been reported to contribute to good flowability properties [20]. It has been reported that increased moisture can inhibit flowability [14], however the moisture content within the powder remained stable throughout recycling in this study.

Image analysis was performed on virgin (cycle 0) and recycled (cycle 7) powder for quantitative evidence of degradation, as shown in Figure 10. The virgin powder contained highly spherical particles. However, larger agglomerated spatter particles were present within the recycled powder despite the inclusion of a two-stage sieving process, post fabrication. Spatter particles within AM powder has been shown within literature to have an unwanted impact on chemical composition [21].

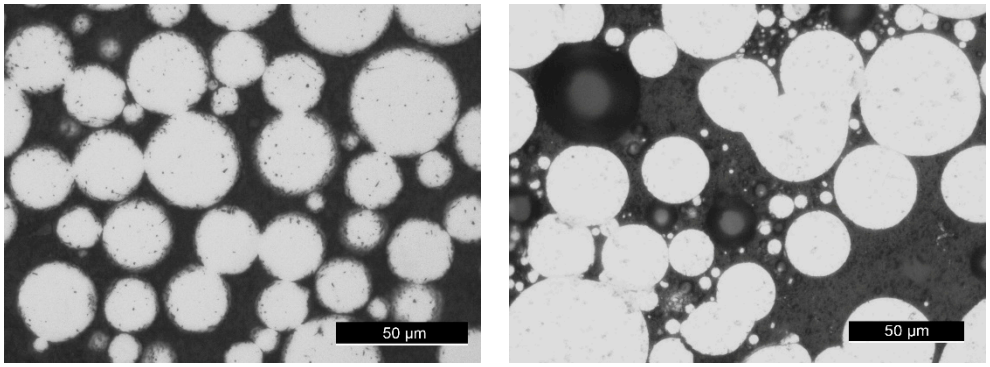

(**a**) (**b**)

Figure 10. 2-dimensnional (2D) cross-sectional images of Ti6Al4V powder at (**a**) cycle 0 (virgin) and (**b**) cycle 7.

The HFR was measured directly at select cycles, to determine the powder's flow properties. The HFR from cycle 0 to cycle 9 decreased from 30 s per 50 g to 23.6 s per 50 g, respectively. Indicating improved flowability during recycling. In addition, H_R and C_I were also used for an indirect measure for powder flowability [3]. Both H_R and C_I decreased during recycling, supporting the conclusion that flowability improved. A number of reasons can be offered to justify the improved flowability property experienced. The reduction of fine particles reported within the PSD analysis can improve the powder flowability during recycling. As fine, small particles inhibit flow due to their increased inter-particle adhesion causing friction. Regarding the other powder characterisations other than compositional analysis, no significant variation from virgin state was present across a nine iteration recycling regime.

The primary hypothesis to be determined from the study is the significance of performing frequent powder characterisation, throughout a recycling regime. The initial condition of the feedstock powder can influence longevity and sustainability. Therefore, it was considered essential to characterise the

initial quantity of powder, dictated by the maximum powder capacity of the supply chamber, prior to manufacture. In addition, results from this study shows that ELI Ti6Al4V powder composition can degrade to go out of specification within a relatively short recycling span. For economical reasoning, an increase in the number of recycle iterations is required. A method to achieve this is could be, prior to purchase, to specify lower levels (well below the ELI thresholds) of interstitial elements within the ELI Ti6Al4V powder. Oxygen content thresholds within the ASTM F136-13 standard does not state a minimum requirement, only a maximum. However, analysis to decide the financially viability may be required as more stringent requirements on composition will increase powder cost. It should be noted that the component to chamber volume ratios reported are low (less than 0.1 for all cases). A regression analysis comparing interstitial composition to build volume ratio (as build volume ratio is representative of scanned area fraction), was attempted no significant trend could be correlated to any satisfactory level. Nevertheless, investigations could be expanded to higher build volume ratios as the relationship between splatter and scanned area fraction could become interesting at higher levels.

5. Conclusions

This work has determined the presence of powder property variation for ELI Ti6Al4V powder due to the implementation of a recycling regime, within a L-PBF process. From cycle 0 to cycle 9, oxygen increased from 0.095 wt% to 0.126 wt%. Additionally, three oxygen data points between cycles 7 and 8 exceeded the maximum oxygen limit of 0.13 wt% whilst complying with the ASTM F136-13. On analysis of the regression model for the oxygen content versus recycle iteration, the determined p-value (7.84×10^{-8}) supported the rejection of the null hypothesis. In relation to the nitrogen and hydrogen content, no clear trend had developed and both elements remained well below their upper threshold limits of the ELI Ti6Al4V alloy.

The PSD curve and cumulative frequency remained relatively stable throughout, when virgin (cycle 0) and cycle 9 powder was compared. This has been confirmed on analysis of the Dv_{10}, Dv_{50} and Dv_{90} values which showed little variance throughout recycling, as shown within Table 5. Highly spherical power particles were observed on inspection of the SEM images throughout recycling. The particle shape analysis quantitatively confirmed this from the mean circularity values present at both the virgin (0.971) and cycle 7 (0.970) powder states.

For the powder flowability, the HFR decreased from 30 s per 50 g at cycle 0 to 23.6 s per 50 g at cycle 9, indicating improved powder flowability. Additionally, H_R and C_I were derived from the bulk and tapped density to indirectly assess the powder's flowability at each recycle iteration. Both flowability indicators showed that the powder remains within the free-flowing powder state throughout recycling, a desirable powder attribute for the L-PBF process.

The largest powder variation that had occurred during recycling was the oxygen content, that showed an upward trend with increasing powder recycles. Most significantly, the three data oxygen data points that exceeded the threshold (0.13 wt%) indicated that a degradation of the ELI Ti6Al4V powder from Grade 23 (but still within Grade 5) had occurred in 9 recycling interactions which is much lower than those reported in other studies [4,17].

To determine the effect that the powder property variation has upon the ELI Ti6Al4V part properties, future work will include mechanical testing upon as-built parts. That will include tensile properties, hardness, density and porosity analysis. Additionally, a more focused assessment of the two-stage sieving process is required. This will involve acquiring multiple powder samples throughout sieving and performing characterisation tests, with a focus upon the chemical compositional analysis.

Author Contributions: Conceptualization, R.H. and S.M.; data curation, R.H., H.W. and S.N.; formal analysis, R.H.; funding acquisition, J.Q. and S.M.; investigation, R.H., H.W. and S.N.; methodology, R.H., H.W. and S.N.; supervision, J.Q. and S.M.; visualization, R.H. and H.W.; writing—original draft, R.H.; writing—review and editing, R.H., H.W., S.N., J.Q., and S.M. All authors have read and agreed to the published version of the manuscript.

Funding: This research was funded by INTERREG VA Programme, managed by the Special EU Programmes Body (SEUPB), as part of the NW CAM project. The APC was funded through the NW CAM project.

Acknowledgments: The North West Centre for Advanced Manufacturing (NW CAM) project is supported by the European Union's INTERREG VA Programme, managed by the Special EU Programmes Body (SEUPB). The views and opinions in this document do not necessarily reflect those of the European Commission or the Special EU Programmes Body (SEUPB). If you would like further information about NW CAM please contact the lead partner, Catalyst, for details.

Conflicts of Interest: The authors declare no conflict of interest.

References

1. Santecchia, E.; Spigarelli, S.; Cabibbo, M. Material Reuse in Laser Powder Bed Fusion: Side Effects of the Laser—Metal Powder Interaction. *Metals* **2020**, *10*, 341. [CrossRef]
2. Kazantseva, N.; Krakhmalev, P.; Yadroitsev, I.; Fefelov, A.; Merkushev, A.; Ilyinikh, M.; Vinogradova, N.; Ezhov, I.; Kurennykh, T. Oxygen and nitrogen concentrations in the Ti-6Al-4V alloy manufactured by direct metal laser sintering (DMLS) process. *Mater. Lett.* **2017**, *209*, 311–314. [CrossRef]
3. Sun, Y.; Aindow, M.; Hebert, R.J. Comparison of virgin Ti-6Al-4V powders for additive manufacturing. *Addit. Manuf.* **2018**, *21*, 544–555. [CrossRef]
4. Thejane, K.; Chikosha, S.; Du Preez, W. Characterisation and Monitoring of Ti6Al4V (Eli) Powder Used in Different Selective Laser Melting Systems. *S. Afr. J. Ind. Eng.* **2017**, *28*, 161–171. [CrossRef]
5. Dawes, B.J.; Bowerman, R. Introduction to the Additive Manufacturing Powder Metallurgy Supply Chain: Exploring the production and supply of metal powders for AM processes. *Technol. Rev.* **2015**, *59*, 243–256. [CrossRef]
6. Spierings, A.B.; Voegtlin, M.; Bauer, T.; Wegener, K. Powder flowability characterisation methodology for powder-bed-based metal additive manufacturing. *Prog. Addit. Manuf.* **2015**, *1*, 9–20. [CrossRef]
7. Sun, P.; Fang, Z.Z.; Zhang, Y.; Xia, Y. Review of the Methods for Production of Spherical Ti and Ti Alloy Powder. *JOM* **2017**, *69*, 1853–1860. [CrossRef]
8. Debroy, T.; Wei, H.; Zuback, J.; Mukherjee, T.; Elmer, J.; Milewski, J.; Beese, A.; Wilson-Heid, A.; De, A.; Zhang, W. Progress in Materials Science Additive manufacturing of metallic components–Process, structure and properties. *Prog. Mater. Sci.* **2018**, *92*, 112–224. [CrossRef]
9. Tang, H.P.; Qian, M.; Liu, N.; Zhang, X.Z.; Yang, G.Y.; Wang, J. Effect of Powder Reuse Times on Additive Manufacturing of Ti-6Al-4V by Selective Electron Beam Melting. *JOM* **2015**, *67*, 555–563. [CrossRef]
10. Cordova, L.; Campos, M.; Tinga, T. Revealing the Effects of Powder Reuse for Selective Laser Melting by Powder Characterization. *JOM* **2019**, *71*, 1062–1072. [CrossRef]
11. Del Re, F.; Contaldi, V.; Astarita, A.; Palumbo, B.; Squillace, A.; Corrado, P.; Di Petta, P. Statistical approach for assessing the effect of powder reuse on the final quality of AlSi10Mg parts produced by laser powder bed fusion additive manufacturing. *Int. J. Adv. Manuf. Technol.* **2018**, *97*, 2231–2240. [CrossRef]
12. Rousseau, J.N.; Bois-Brochu, A.; Blais, C. Effect of oxygen content in new and reused powder on microstructural and mechanical properties of Ti6Al4V parts produced by directed energy deposition. *Addit. Manuf.* **2018**, *23*, 197–205. [CrossRef]
13. Carrion, P.E.; Soltani-Tehrani, A.; Phan, N.; Shamsaei, N. Powder Recycling Effects on the Tensile and Fatigue Behavior of Additively Manufactured Ti-6Al-4V Parts. *JOM* **2019**, *71*, 963–973. [CrossRef]
14. Quintana, O.A.; Alvarez, J.; McMillan, R.; Tong, W.; Tomonto, C. Effects of Reusing Ti-6Al-4V Powder in a Selective Laser Melting Additive System Operated in an Industrial Setting. *JOM* **2018**, *70*, 1863–1869. [CrossRef]
15. Sutton, A.T.; Kriewall, C.S.; Karnati, S.; Leu, M.C.; Newkirk, J.W. Characterization of AISI 304L stainless steel powder recycled in the laser powder-bed fusion process. *Addit. Manuf.* **2020**, *32*, 100981. [CrossRef]
16. Powell, D.; Rennie, A.E.W.; Geekie, L.; Burns, N. Understanding powder degradation in metal additive manufacturing to allow the upcycling of recycled powders. *J. Clean. Prod.* **2020**, *268*, 122077. [CrossRef]
17. Denti, L.; Sola, A.; Defanti, S.; Sciancalepore, C.; Bondioli, F. Effect of Powder Recycling in Laser-based Powder Bed Fusion of Ti-6Al-4V. *Manuf. Technol.* **2019**, *19*, 190–196. [CrossRef]
18. Seyda, V.; Kaufmann, N.; Emmelmann, C. Investigation of Aging Processes of Ti-6Al-4V Powder Material in Laser Investigation of aging processes of Ti-6Al-4V powder material in laser melting. *Phys. Procedia* **2012**, *39*, 425–431. [CrossRef]
19. Park, S.B.; Road, B.; Kingdom, U. Investigating the effects of multiple re-use of Ti6Al4V powder in additive manufacturing. *Renishaw PLC* **2016**, 1–10.

20. Brika, S.E.; Letenneur, M.; Dion, C.A.; Brailovski, V. Influence of particle morphology and size distribution on the powder flowability and laser powder bed fusion manufacturability of Ti-6Al-4V alloy. *Addit. Manuf.* **2020**, *31*, 100929. [CrossRef]
21. Obeidi, M.A.; Mussatto, A.; Groarke, R.; Vijayaraghavan, R.K.; Conway, A.; Kaschel, F.R.; McCarthy, E.; Clarkin, O.; O'Connor, R.; Brabazon, D. Comprehensive assessment of spatter material generated during selective laser melting of stainless steel, Mater. *Today Commun.* **2020**, *25*, 101294. [CrossRef]